Volume 6, Issue 2, 2016, 1099-1103 ISSN 2069-5837

Biointerface Research in Applied Chemistry

www.BiointerfaceResearch.com

Original Research Article Open Access Journal

Received: 21.02.2016 / Revised: 10.03.2016 / Accepted: 13.03.2016 / Published on-line: 20.03.2016

Helical microtubules of nanostructured cobalt oxide for electrochemical energy storage applications

Funda Ersoy Atalay [1,*], Harun Kaya [1], Dilek Asma [2], Alper Bingöl [1]

[1]Inonu University, Science and Art Faculty, Department of Physics, Malatya 44280, Turkey
[2]Inonu University, Science and Art Faculty, Department of Biology, Malatya 44280, Turkey

*corresponding author e-mail address: ***funda.atalay@inonu.edu.tr***

ABSTRACT

In this study, Co_3O_4 nanostructured porous microtubes were prepared via chemical precipitation onto *Aquaspirillum bengal* bacteria in an aqueous solution. The morphological properties of the synthesized material were studied using scanning electron microscopy (SEM). The diameter of the Co_3O_4 micro tubes is approximately 0.8 µm, and the length is 4 µm. The Brunauer–Emmett–Teller (BET) surface area was determined to be 87.07 m^2/g. The nitrogen adsorption and desorption isotherm displayed properties associated with a typical type IV isotherm. The electrochemical properties of the produced material were studied using cyclic voltammetry (CV), long-term charge/discharge analysis and impedance spectroscopy (EIS).

Keywords: *cobalt oxide, supercapacitor, bacteria, Aquaspirillum bengal, nanoparticle.*

1. INTRODUCTION

Recently, biological microorganisms have been used as templates for the fabrication of inorganic functional materials [1, 2]. Among them, some bacterial structures are particularly attractive biotemplates due to their surface-layer proteins. The morphological properties of these surface-layer proteins make them an ideal matrix for biotemplating in the direct chemical synthesis of nanostructures. Previous studies have demonstrated how porous metal oxide nanostructures, particularly Co_3O_4, can be extensively used as supercapacitor electrode materials [2, 3].

Spirilla are commonly found in freshwater and marine environments. They have a helical shape, and their DNA base composition is 51% mol guanine and cytosine. As reported by Kumar *et al.* [4], the genus Spirillum was isolated from a freshwater pond in West Bengal and is in the *Aquaspirillum* genus. The strain was named *Aquaspirillum bengal* in the American Type Culture Collection under the number 27641 [4]. This species is unique in having an unusually high temperature for optimal growth of 41°C, forming water-soluble pigments from tyrosine and tryptophan, and possessing several other nutritional, biochemical, and serological characteristics [4]. It has a cell diameter of 0.9 to 1.2 µm, which is similar to those of *A. serpens* and *A. putridiconchylium*. *A. bengal* is a motile bacteria owing to the presence of a bipolar flagellum at each end of the cell [5]. It is Gram-negative and chemo-organotrophic. Gram-negative cell walls are very strong structures and can withstand ~3 atm of turgor pressure. They exhibit a remarkable resistance to high temperatures and pHs and have the ability to expand to several times their normal surface area [6]. It is thought that having these remarkable features arises from the S-layer of the bacteria. It is well known that most bacteria (such as *Bacillus* and *Deinococcus)* have S-layer proteins at their outer surface. *A. bengal* also possesses two superimposed hexagonal S-layer proteins. The underlying layer is attached to the lipopolysaccharide of the outer membrane, and the second layer is attached directly to the first layer [7]. Schultze-Lam *et al.* [8] reported that S-layers of bacteria may induce precipitation of minerals. This led to the idea for their use as templates in the formation of regular arrays of metal clusters, as required in molecular electronics and nonlinear optics [9]. We have recently also reported that S-layer proteins have advantages that include the production of metal oxide nanostructures with a high surface-to-volume ratio [2]. The tubular structure and Gram-negative properties of *A. bengal* result in a high tolerance towards metals, a high S-layer metal binding potential and intracellular metal uptake capabilities. Therefore, in this study, we use the *A. bengal* bacteria to obtain nanostructured helical microtubules, which were then used as the active material in a supercapacitor electrode. The material annealed at 360°C exhibits a highest BET surface area of 87.07 m^2/g. The maximum specific capacitance of Co_3O_4 electrode has a 723 F/g at 2 mV/s, which is comparatively higher than previously reported values [10].

2. EXPERIMENTAL SECTION

Previously, we have reported a chemical precipitation method to obtain nanostructured metal oxide using biological microorganisms [2, 11]. A similar procedure was applied to the *A. bengal* bacteria in this work. The *A. bengal* bacteria used in this work were procured from ATCC (American Type Culture Collection), freeze-dried and stored between 2°C to 8°C in a refrigerator. Gram negative *A. bengal* (ATCC 27641) was cultured in PSB (peptone succinate broth) at pH 7.2 containing 1.0 g of $(NH_4)_2 \cdot SO_4$, 1.0 g of $MgSO_4 \cdot 7H_2O$, 2.0 mg of $MnSO_4 \cdot H_2O$, 2.0 mg of $FeCl_3 \cdot 6H_2O$, 1.68 g of succinic acid, and 5.0 g of peptone

in1000 ml of distilled water. The pH was adjusted to 7.2 using 0.1 M KOH, and the media were sterilized at 121°C at a pressure of 1 atm for 15 min. *A. bengal* was grown in an agitation incubator at 150 rpm and 41°C for 24 hours. Approximately 6 ml of activated cultures was transferred into 250-ml flasks containing 50 ml of PSB. Inoculated Erlenmeyer flasks were incubated at 41°C for 48 h. Then, the bacterial cultures were isolated by centrifugation at 9000 rpm at 4°C for 20 min. The pellets were washed three times with de-ionized water and then once with ethanol to remove any traces of the media before the cell suspensions were harvested.

First, 200 ml of a 200 mM $CoCl_2$ solution was mixed with the cell suspension of *A. bengal* at a rate of 10 ml/min using a burette to obtain a porous metal oxide material. The mixture was continuously agitated at 170 rpm at room temperature. After shaking for 30 minutes, 100 ml of a 25 mM $NaBH_4$ solution was also added to the mixture at a rate of 10 ml/min. Agitation was continued at 170 rpm for 24 h, followed by centrifugation and collection of the precipitate. The CoO(OH)/bacteria precipitate was washed thoroughly two times with de-ionized water and then once with ethanol. The formed tubular precipitate was dried for 24 h in a vacuum oven at 60°C. The produced nanostructures were heated from room temperature to various annealing temperatures (120°C-400°C) in air at a rate of 1°C/min and held at the final temperature for 12 h. This process was followed by cooling to room temperature at a rate of 1°C/min.

The surface areas of the material obtained at various annealing temperatures were also studied by BET analysis using a Micromeritics Gemini VII 2390t. The pore size distribution was determined by the Barrett-Joyner-Halenda (BJH) method. Thermo gravimetric analysis (TGA) measurements were performed in air by heating the samples from room temperature to 950°C at a ramp rate of 10°C/min using a Shimadzu TGA-50 thermo gravimetric analyzer. The crystal structure and orientation was determined using a Rigaku-Radb X-ray diffractometer (XRD) equipped with CuKα radiation. The chemical nature was studied with X-ray photoelectron spectroscopy (XPS; SPECS EA 300). The morphologies of materials were examined using scanning electron microscopy (SEM; LEO-EVO-40) and transmission electron microscopy (TEM; JEOL JSM 7001F).

The electrode fabricated from the metal oxide precipitated bacteria was prepared according to the following steps. The nanostructured Co_3O_4 microtubes (75%), acetylene black (15%) and PVDF (10%) were ground and mixed in a Zr_2O_3 mortar until a homogenous mixture was obtained. Subsequently, a drop of NMP was added to this mixture. A 6.25 mg aliquot of this mixed material was spread on a Ni foam sheet and dried for 12 h in a vacuum oven at 90°C. The Ni foam supporting material was compressed at a pressure of 5 MPa for 5 min and was used as the working electrode. A reference electrode was composed of Ag/AgCl (with ceramic frit, ALS, saturated KCl, and 45 mV versus SCE at 20°C). Platinum was used as auxiliary electrodes. All of the electrochemical experiments were carried out in a three-electrode cell configuration in 6 M KOH as the electrolyte solution. Electrochemical investigations included cyclic voltammetry (CV) measurements, galvanostatic charge–discharge tests and electrochemical impedance spectroscopy (EIS) using a Gamry Reference 3000 potentiostat/galvanostat/ZRA.

3. RESULTS SECTION

The TGA weight loss curves over a temperature range of 25°C to 1000°C for the pure bacteria and metal-precipitated bacteria are shown in Figure 1. A steady weight loss from room temperature to 125°C in the TGA data is attributed to water evaporation. Subsequent steady weight loss from 125°C to 300°C is caused by the continual expulsion of water and ethanol from the material as a result of condensation reactions. Steady weight loss from 300°C to 600°C is attributed to the degradation of the bacteria.

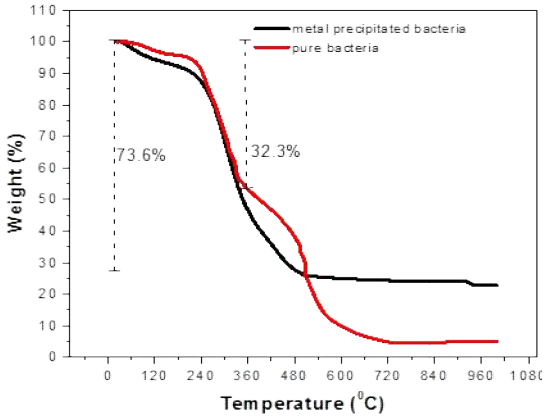

Figure 1. TGA analysis for pure *A. bengal* and precipitated metal onto *A. bengal.*

As reported by Wang et al. [12], TGA measurements of nano-CoOOH illustrated that after the initial loss of moisture accumulated in the nanostructured CoOOH, the weight loss from 200°C to 400°C was due to a gradual decomposition of the CoOOH. The Co_3O_4 formed via the decomposition of CoOOH, and O_2 and H_2O were also produced when the temperature rose above 300°C. Then, CoO was formed at higher temperatures. This observation is in agreement with our results. The TGA curve belonging to the metal-precipitated bacteria illustrates that a gradual decomposition of CoOOH and degradation of bacteria occurred together over the temperature range of 200°C to 500°C with a gradual weight loss of ~73.6%. Above 500°C, the curve shows no further weight loss, indicating a composition of 26.4% inorganic matter, most of which is likely metal oxide above 500°C. The weight fraction of Co_3O_4 in the metal precipitated sample may be less than 26.4% because of the intrinsic inorganic components of the pure bacteria e.g., C, N, K, and S [13]. The TGA result for pure bacteria indicates that the amount of inorganic residue for *A. bengal* was 53.2 % and 32.2% at 360°C and 500°C, respectively.

Figure 2a shows the N_2 adsorption-desorption isotherms and corresponding BJH pore size distribution curves for the Co_3O_4 materials obtained at various annealing temperature. The samples annealed at 300°C and above exhibit a typical type IV isotherm

corresponding to a mesoporous sample. The effect of the annealing temperature on the pore size is clearly observed in the BJH pore size distribution curves (inset). The sample annealed at 360°C exhibited two main nitrogen adsorption of pore volume versus pore diameter (Figure 2b). The smaller and sharper peak is assigned to pores with diameters that vary between 1.8 and 4 nm. The peak maximum is 2.6 nm. The larger and broader peak is assigned to pores with diameters varying between 17.4 nm and 19 nm. The maximum of this peak is 14.3 nm. The BET surface area versus temperature curve also indicates that the best temperature to achieve mesoporosity is 360°C. The BET surface area and pore volume for the sample annealed at 360°C are calculated to be 87.07 m^2 g^{-1} and 0.179 cm^3 g^{-1}, respectively.

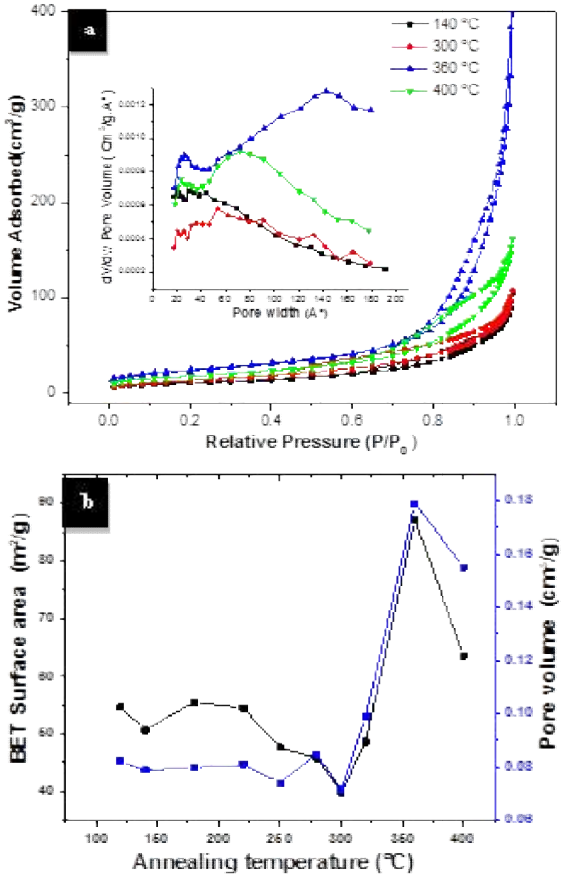

Figure 2. a) Nitrogen adsorption isotherm of nanostructured Co_3O_4 materials. Inset shows the pore size distribution of Co_3O_4 nanostructures b) BET surface area and pore volume as a function of annealing temperature.

Figure 3a shows the XRD profiles for the metal precipitated bacteria before and after the annealing process at 360°C. Before the annealing process, the structure consists of only pure CoO(OH) peaks. The newly appeared peaks after the annealing process, which are located at 2θ= 31.32°, 36.86°, 44.72°, 59.44° and 65.32°,are assigned to a cubic spinel Co_3O_4 structure, as found in JCPDS card file No.65-3103. The Figure 3b shows XPS spectra of metal percipiated then annealled sample at 360°C in the 0-1200 eV. The average atom concentration elements on the surface of sample was calculated from XPS peak areas. The major peaks in the spectra identified by XPS were Co, C, and O, with minor peaks of Cl, S and N peaks whose composition and elemental ratios are presented in the legend of the respective graph. The minor peaks can be attributed to functional groups on the outermost bacterial cell. Co2p XPS spectra consists of two main $2p_{1/2}$, $2p_{3/2}$, spin-orbit lines, at 793.9 eV and 778.3 eV, separated by about 15.6 eV, which agree well with literature [14]. This result support the Co_3O_4 the presence of tetrahedral Co cations, characteristic of the spinel Co_3O_4 (111) structure.

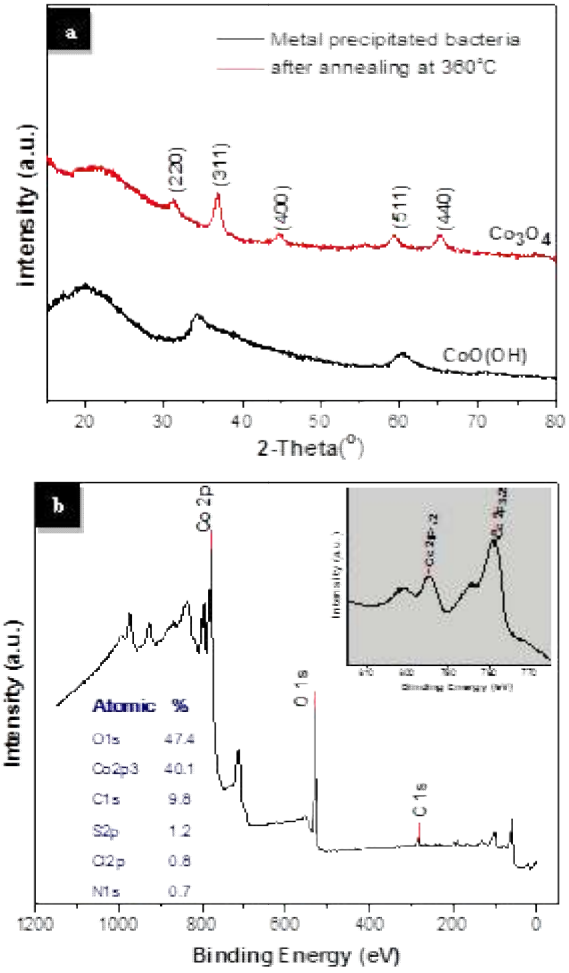

Figure 3. a) XRD spectrum for precipitated material and nanostructured Co_3O_4 material after annealing processes at 360ºC. b) XPS spectrum for chemically precipitated then annealled sample. The inset shows Co $2p_{3/2}$ XPS spectra.

The stack of bare *A. bengal is* seen in Figure 4a.

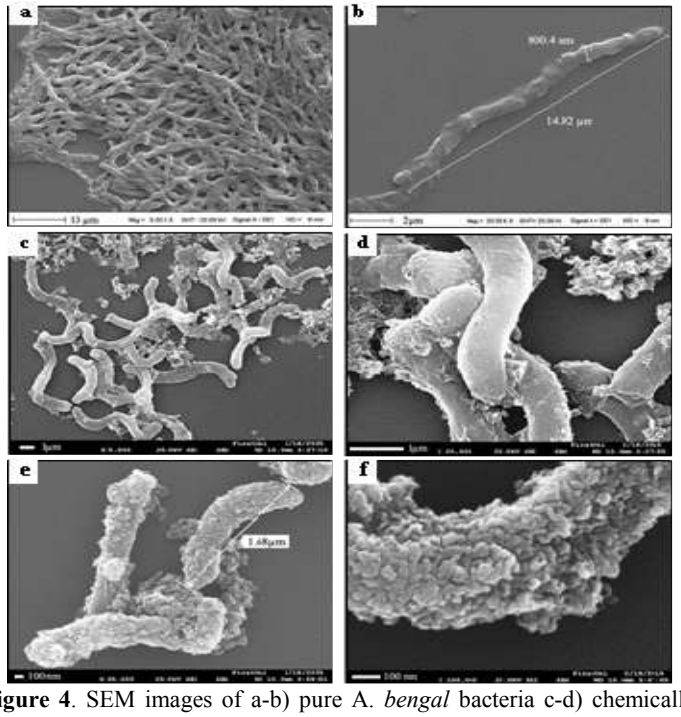

Figure 4. SEM images of a-b) pure A. *bengal* bacteria c-d) chemically precipitated sample on *A. bengal* e-f) nanostructured Co_3O_4 sample after annealing processes at 360ºC.

The helix-shaped bacteria have a length of approximately 15 µm and a diameter of 800 nm, as shown in Figure 4b. The metal-precipitated bacteria are seen in Figure 4c and d. After heat treatment at 360°C, the structure of the helix became granulated, and the length of helix shortened (Figures 4e and 4f).

Figure 5 shows typical CV curves for prepared Co_3O_4-precipitated bacteria over a potential window of 0 to 0.5 V (versus Ag/AgCl) at different scan rates. The shapes of the CVs are non-rectangular, which is due to the pseudocapacitance and is based on the redox mechanism of the different Co oxidation states [15, 16]:

$$CoOOH+OH^- \leftrightarrow CoO_2+H_2O+e^- \quad (1)$$

$$Co_3O_4+H_2O+OH^- \leftrightarrow 3CoOOH+e^- \quad (2)$$

The anodic and corresponding cathodic peaks for a 10 mV/s scan rate are 0.36 V/0.24 V and 0.31 V/0.16 V for Co^{2+}/Co^{3+} (corresponding to Equation (1)) and Co^{3+}/Co^{4+} (corresponding to Equation (2)) redox transitions, respectively (Figure 5). The redox current increases with the scan rate, which suggests that good reversibility exists for a fast charge–discharge response. The specific capacitance of the Co_3O_4 electrode is computed from the CVs using the following formula [17]:

$$C_s = \frac{\int I dV}{s \times \Delta V \times m} \quad (3)$$

where I is the current, s is the scan rate, ΔV is the potential window and m is the active material mass. The maximum specific capacitance is 723 F/g at 2 mV/s (as shown in the inset of Figure 5). When the scan rate is increased to 5 mV/s, the specific capacitance of the Co_3O_4 electrode is 159 F/g. The specific capacitance value decrease with the increasing scan rate. This is due to limited ions movement at the high scan rate.

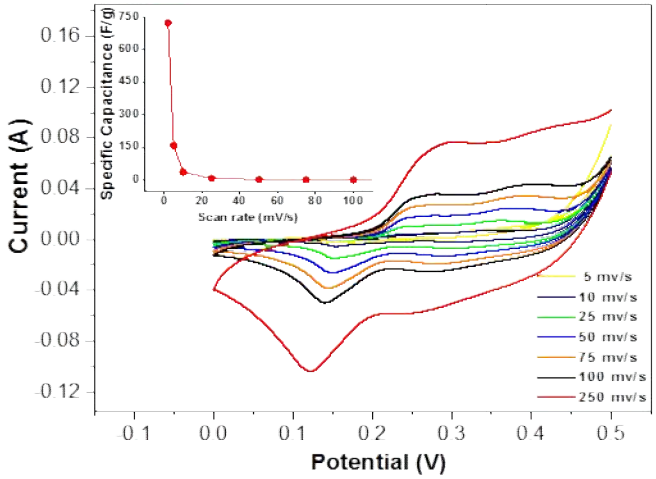

Figure 5. CV curves of Co_3O_4 electrodes at different scan rates. The inset shows specific capacitance as a function of the scan rate.

Figure 6 shows the galvanostatic cycle charge-discharge test for Co_3O_4-precipitated bacteria electrode at a rate of 0.8 A/g. The specific capacitance is also evaluated from according to the following equation [17]:

$$C_s = \frac{I \times \Delta t}{m \times \Delta V} \quad (4)$$

where I is the discharge current, Δt is the discharge time, ΔV is the potential drop in the discharge progress and m is the active mass of the electrode. The capacitance variation of the supercapacitor was investigated over 2500 cycles, as shown in the inset of Figure 6.

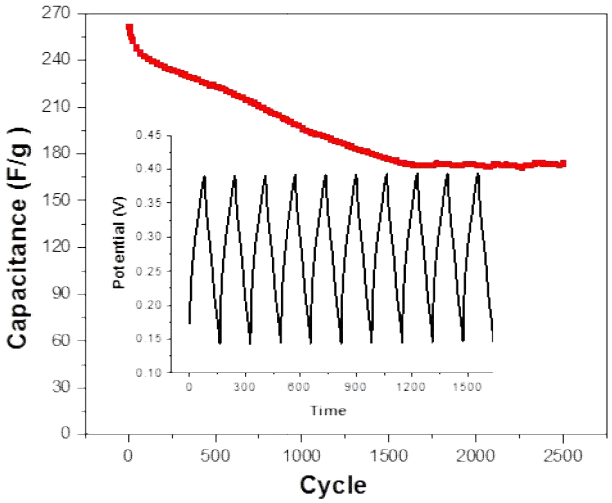

Figure 6. The variation of specific capacitance as a function of cycle number of Co_3O_4 electrode. The inset shows the ten cyclic charge-discharge curves.

It was observed that the capacitance of the supercapacitor decreased gradually with the increase in the number of cycles. The coulombic efficiency increased with the number of cycles. The initial capacitance value was 262 F/g. After 1000 and 1635 continuous charge-discharge cycles, these values decreased to 197 F/g and 174 F/g, respectively. Then, the system stabilized and the capacitance values did not change. A capacitance retention of approximately 75% of the initial capacitance was seen after 1000 cycles. The specific capacitance value obtained from the charge-discharge test agreed well with the CV results of 5mV/s.

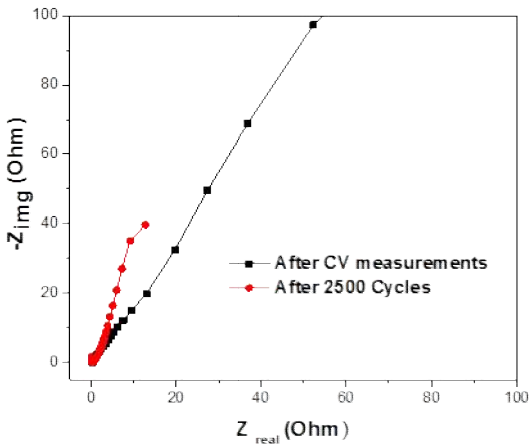

Figure 7. Nyquist plots of Co_3O_4 electrode at open circuit potential in 6M KOH solution.

The electrochemical impedance spectroscopy (EIS) measurements were performed by applying a sinusoidal wave with an amplitude of 1 mV over a frequency range from 100 kHz to 5 MHz. Figure 7 shows the Nyquist graph of the AC impedance for the Co_3O_4 electrode after the CV measurements and long-term cycling at an open circuit potential. The contact resistance between the electrolyte and the electrode material is approximately 213 mΩ, which shows changes by 10% after 2500 cycles. This indicates that the Co_3O_4 nanocomposites may enable much easier charge transfer at the electrode/electrolyte interface as a result of their good electrical conductivity. After 2500 continuous cycles, the obvious decrease in charge transfer

resistance over the middle frequency range and a 75 degree sloping straight line over the low frequency range are good electrochemical capacitive features, which are typical characteristics of the porous electrode structure.

4. CONCLUSIONS

In summary, we have successfully produced nanostructured porous Co_3O_4 using *A. bengal* bacteria via a chemical precipitation method. The microorganisms, especially the bacteria, contained S-layers that are a most advantageous biotemplate for obtaining nanostructures due to their low generation times, easy growth conditions and different shapes and sizes. The excellent properties of the produced Co_3O_4 material, including a high surface area and a porous structure, lead to good electrochemical performance, such as specific capacitance and a long cycle life when used as an electrode active material for energy storage.

5. REFERENCES

[1] Rehman A., Majeed M.I., Ihsan *A.,* Hussain *S.*Z., Rehman S.U., Ghauri M.A., Khalid Z.M., Hussai I., Living fungal hyphae-templated porous gold microwires using nanoparticles as building blocks, *Journal of Nanoparticle Research,* 1, 6747–6754, **2011.**

[2] Atalay F.E., Asma D., Kaya H., Ozbey E., The fabrication of metal oxide nanostructures using *Deinococcus radiodurans* bacteria for supercapacitor, *Materials Science in Semiconductor Processing*, 38, 314–318, **2015.**

[3] Dua W., Liu R., Jiang Y., Lu Q., Fan Y., Gao F., Facile synthesis of hollow Co_3O_4 boxes for high capacity supercapacitor, *Journal of Power Sources*, 227, 101-105, **2013.**

[4] Kumar R., Banerjee A.K., Bowdre J.H., McElroy L.J., Krieg N.R., Isolation, Isolation, Characterization, and Taxonomy of *Aquaspirillum bengal* sp.nov., *International Journal of Systematic and Evolutionary Microbiology,* 24, 453-458, **1974.**

[5] Yoon J.H., Kang S.J., Park S., Lee S.Y., Oh T.K., Reclassification of Aquaspirillumitersonii and *Aquaspirillum peregrinum as Novispirillum itersonii* gen. nov., comb. nov. and *Insolitispirillum peregrinum* gen. nov. comb. nov., *International Journal of Systematic and Evolutionary Microbiology,* 57, 2830–2835, **2007.**

[6] Beveridge T.J., Structures of Gram-Negative Cell Walls and Their Derived Membrane Vesicles, *Journal of Bacteriolgy,* 181, 4725–4733, **1999.**

[7] Stewart M., Murray R.G.E., Structure of the regular surface layer of *Aquaspirillum serpens* MW5, *Journal of Bacteriolgy*, 150, 348-357, **1982.**

[8] Schultze-Lam S., Harauz G., Beveridge T.J., Participation of a cyanobacterial S-layer in fine-grain mineral formation, *Journal of Bacteriolgy,* 174, 7971-7981, **1992.**

[9] Sára M., Sleytr U.B., S-Layer proteins**,** *Journal of Bacteriolgy,* 182, 859–868, **2000.**

[10] Sankapal B.R., Gajare H.B., Karade S.S., Dubal D.P., Anchoring cobalt oxide nanoparticles on to the surface multiwalled carbon nanotubes for improved supercapacitive performances, *RSC Advances*, 5, 48426-48432, **2015.**

[11] Atalay F.E., Asma D., Aydogmus E., Turanci H., Kaya H., The Fabrication of NiO Microtubes Using *Bacillus subtilis* Bacteria, *Acta Physica Polonica A***,** 125, 235-237, **2014.**

[12] Wang J.W., Kuo Y.M., Synthesis of Nanosized Zinc-Doped Cobalt Oxyhydroxide Parties by a Dropping Method and Their Carbon Monoxide Gas Sensing Properties, *Journal of Nanomaterials,* 136145-13614553, **2013.**

[13] Shim H.W., Jin Y.H., Seo S.D., Lee S.H., Kim D.W., Highly Reversible Lithium Storage in Bacillus subtilis-Directed Porous Co_3O_4 Nanostructures, *ACS Nano,* 5, 443-449, **2011.**

[14] Hongyan X., Libo G., Qiang Z., Junyang L., Jiangtao D., Xiujian C., Jun T., Chenyang X., Preparation Method of Co_3O_4 Nanoparticles Using Degreasing Cotton and Their Electrochemical Performances in Supercapacitors, *Journal of Nanomaterials,* 723057-723065, **2014.**

[15] Barbero C., Planes G.A., Miras M.C., Redox coupled ion exchange in cobalt oxide films, *Electrochemistry Communications,* 3, 113-116, **2001.**

[16] Tummala R., Guduru R.K., Mohanty P.S., Nanostructured Co_3O_4 electrodes for supercapacitor applications from plasma spray technique, *ournal of Power Sources,* 209, 44–51, **2012.**

[17] Krishnamoorthy K., Veerasubramani G.K., Radhakrishnan S., Kim S.J., Supercapacitive properties of hydrothermally synthesized sphere like MoS_2 nanostructures, *Materials Research Bulletin,* 50, 499–502, **2014.**

6. ACKNOWLEDGEMENTS

This work was supported by TUBITAK under project number MAG-113M335.